Journal of Materials Chemistry B

Tensile properties and in vitro degradation of P(TMC-co-LLA) elastomers

Journal:	*Journal of Materials Chemistry B*
Manuscript ID:	TB-ART-01-2015-000202.R2
Article Type:	Paper
Date Submitted by the Author:	28-Apr-2015
Complete List of Authors:	Cork, Jorja; The University of Queensland, School of Chemistry and Molecular Biosciences; The University of Queensland, Australian Institute for Bioengineering and Nanotechnology (AIBN) Whittaker, Andrew; University of Queensland, Australian Institute for Bioengineering and Nanotechnology Cooper-White, Justin; The University of Queensland, Australian Institute for Bioengineering and Nanotechnology (AIBN) Grondahl, Lisbeth; The University of Queensland, School of Chemistry and Molecular Biosciences

Tensile properties and *in vitro* degradation of P(TMC-co-LLA) elastomers

Jorja Cork[a,b], Andrew K. Whittaker[b], Justin J. Cooper-White*[b,c,d], Lisbeth Grøndahl*[a]

[a] School of Chemistry and Molecular Biosciences, University of Queensland, Brisbane, Queensland 4072, Australia

[b] The Australian Institute for Bioengineering and Nanotechnology, University of Queensland, Brisbane, Queensland 4072, Australia

[c] School of Chemical Engineering, University of Queensland, Brisbane, Queensland 4072, Australia

[d] CSIRO, Division of Materials Science and Engineering, Clayton, Victoria 3169 Australia

Corresponding authors:

Professor Justin J Cooper-White

Phone: +61 7 334 63858 Email: j.cooperwhite@uq.edu.au

Associate Professor Lisbeth Grøndahl

Phone: +61 7 336 53671 Fax: +61 7 336 54299 Email: l.grondahl@uq.edu.au

Abstract

P(TMC-co-LLA) elastomers have shown great potential for various biomaterials applications. This study investigated properties key to such applications. Six statistical copolymers with 16 to 49 mol% TMC were synthesized and it was found that the LLA sequence length changed from 14 to 3 for the copolymer series while the $\bar{M}_n$ decreased from 63 to 31 kg/mol with increasing TMC content. The thermal properties showed lower T_g values with increasing TMC content which agreed with the Fox equation. Solvent cast films exhibited Young's modulus values between 2.8 and 271 MPa, ultimate tensile strength of 0.6 – 15.5 MPa and elongation at failure from 356 to 1287 %. *In vitro* degradation in PBS at 37 ^{o}C over 34 weeks demonstrated an induction period of 9 weeks during which the water content was minimal for all copolymers. Copolymer films with 21 or greater mol% TMC were found to undergo homogeneous bulk degradation, while the P(TMC_{16}-co-LLA_{84}) films underwent heterogeneous bulk degradation.

Introduction

Polyester carbonates offer a wide range of material properties and have been investigated for a vast number of applications including vascular grafts, heart tissue engineering, drug delivery, nerve-end guides, wounds dressings, biomaterial coatings and as biodegradable internal fracture fixation devices.[1-4] The synthesis of polyester carbonates is commonly performed via ring-opening polymerisation (ROP) in the presence of a catalyst and/or initiating species. A number of different polymer compositions and topologies have been investigated, however, statistical linear polyester carbonate of ε-caprolactone (εCL), glycolide (GA), *D,L*-lactide (DLLA), *L*-lactide (LLA) or *D*-lactide (DLA) with trimethylene carbonate (TMC) have received considerable attention. Specifically, statistical P(TMC-co-LLA) copolymers have been investigated with respect to their mechanical properties,[5-10] and their degradation *in vitro*[4,11-15] and *in vivo*.[16]

In vitro and *in vivo* compatibility of P(TMC-co-LLA) elastomers have been evaluated. Specifically, the P(TMC_{50}-co-LLA_{50}) copolymer was found to display very low haemolytic ratios *in vitro* indicating good haemolytic properties.[17] Furthermore, when implanted into rats it displayed very low cytotoxicity and high histo-compatibility and this study concluded that the material is suitable for cardiovascular stent/stent coating material applications.[16] UV-crosslinked P(TMC-co-LLA) copolymers were found to be non-toxic and to support mesenchymal stem cell attachment and proliferation *in vitro,* as well as induce growth of artificial blood vessels *in vivo* when implanted into the peritonial cavity of rats.[18] Gamma radiation crosslinked degradable P(TMC_{56}-co-LLA_{44}) elastomeric scaffolds were likewise found to support mesenchymal stem cell attachment and proliferation *in vitro*.[19] From these studies it is clear that P(TMC-co-LLA) elastomers have great potential in biomaterials applications. Key to such applications, in addition to the biological response, is the mechanical properties, as well as rates and mechanisms of degradation.

With regards to degradation of P(TMC-co-LLA) elastomers, there is however some discrepancy in the literature. There have been a number of studies detailing the *in vitro* degradation of P(TMC-co-LLA) copolymers in PBS buffer. One study investigated the effect of molar composition and chain microstructure on the *in vitro* degradation behavior.[4] The differences found translated into different drug release behavior with the random amorphous copolymers displaying a regular drug release process.[20] In terms of evaluation of the degradation mechanism and preferential degradation of the different copolymer segments,

one study found preferential degradation of the LLA units,[12] while another study found that the degradation rate increasing with increased TMC content and furthermore established that the polymers were bulk degrading.[11] Bulk degradation was confirmed in a recent study which also found that the T_g was reduced and the crystallinity increased as a function of degradation time.[14] These studies investigated only two or three molar compositions of the P(TMC-co-LLA) copolymers and the focus has been on melt processed materials. Considering the vast range of solvent processing techniques used in fabrication of biomaterials, there is a clear need to evaluate in more detail the degradation of such materials, as well as to further the understanding of the dominant degradation mechanism.

The current study seeks to broaden the understanding of the mechanism of degradation of P(TMC-co-LLA) films. This is achieved through synthesis and physicochemical characterisation of six copolymers of 16 – 49 % TMC content with respect to structure, molecular weight and thermal properties. Solvent cast films are evaluated for their thermal and mechanical properties. Furthermore, a detailed *in vitro* degradation study in PBS monitoring water uptake and mass loss, as well as changes to molecular weight and thermal properties during a 34 week degradation study, allowed for a thorough understanding of the degradation mechanism to be developed.

Experimental

Materials

Trimethylene carbonate (TMC) was purchased from Richman Chemicals, USA and (3*S*)-*cis*-3,6-dimethyl-1,4-dioxane-2,5-dione (LLA) was from Sigma-Aldrich. Both monomers were recrystallised from ethyl acetate prior to use. Stannous octoate ($Sn(Oct)_2$) and Sigmacote® were from Sigma-Aldrich. Phosphate buffered saline (PBS) was from Lonza, USA. All solvents were of HPLC grade and MilliQ water was used throughout.

Methods

Copolymerisations of LLA and TMC were performed via ring-opening polymerisation (ROP) in the bulk using $Sn(Oct)_2$ as the catalyst using a method adapted from Pego *et al*.[21] All glassware was freshly silanised with Sigmacote® and dried overnight at 90 ^{o}C before use. All freshly silanised glassware and recrystallised monomers were stored under an inert nitrogen

atmosphere in a glove box prior to use. Reactions were carried out in a glove box according to the following procedure: monomer(s) were added to each reaction vessel, along with 2×10^{-4} mol of $Sn(Oct)_2$ per mol of monomer as a solution in dry dichloromethane (DCM). The solution was left for 30 minutes for the DCM to evaporate and then sealed and heated with stirring on a heating mantle at 130 ± 2 ^{o}C for 70 - 139 hours. Upon completion of each reaction the copolymer product was allowed to cool, dissolved in a minimal volume of DCM and precipitated dropwise into a ten-fold volume of cold methanol with vigorous stirring. The purification step was repeated and each copolymer product was dried under reduced pressure in a vacuum desiccator at room temperature until constant weight was achieved. The copolymers are named P(TMC_x-co-LLA_y), where *x* refers to the mol% incorporation of TMC and *y* refers to the mol% incorporation of LLA.

Solvent casting of the copolymers was done by dissolution in a minimal amount of solvent, either propylene glycol monomethyl ether acetate (PGMEA) or PGMEA and DCM, at room temperature. The solvent mixture used during the film casting was chosen depending on the solubility of each individual copolymer sample. The copolymers with low TMC content (16 and 21 mol% TMC) were dissolved in a solvent mixture of PGMEA and DCM, while the remaining copolymers were dissolved in PGMEA. The solution concentration before casting ranged from 10 - 33 w/w %. Upon dissolution, each solution was poured into a 70 mm diameter glass petri dish and left on a level surface in a fumehood to cast. The films were then further dried in a vacuum oven at room temperature. All films were dried for a minimum of 12 days before undergoing mechanical testing.

Physicochemical characterisation

^{1}H nuclear magnetic resonance (NMR) spectroscopy were run on a Bruker AVANCE 300 MHz operating at 300.13 MHz. Experiments were performed with a standard Bruker 5 mm BBO gradient probe. $CDCl_3$ was used as the solvent and spectra are referenced to the solvent signal at 7.24 ppm. The LLA mol% incorporation, the average block lengths of LLA ($\bar{L}_{LLA}$) were calculated from the ^{1}H NMR spectra according to a published procedure.[21]

Gel permeation chromatography (GPC) was done on a Waters Alliance 2690 Separations Module to determine the mass average and number average molecular-weight ($\bar{M}_w$ and $\bar{M}_n$ respectively), and dispersity ($Đ_M$). Copolymer samples (5 - 10 mg) were dissolved in 2 mL THF and filtered through a 0.45 μm filter. HPLC grade tetrahydrofuran was used as eluent at a flow rate of 1 mL/min. Three 7.8 × 300 mm Waters Styragel GPC columns were connected

in series, comprising 2 linear Ultrastyragel and one Styragel HR3 column. Polystyrene standards ranging from 2,000 – 0.517 kg/mol were used for calibration.

Differential scanning calorimetry (DSC) was run on a Mettler Toledo Differential Scanning Calorimeter, DSC 1 STAR^e system. The instrument was calibrated using the melting temperatures of indium (429.4 K) and zinc (692.5 K) and their heats of fusion. Samples (7 - 12 mg) were placed in aluminium pans which were sealed (hindering escape of any residual solvent) and run at a heating/cooling rate of ±10 ^{o}C/min. Samples underwent a 5 segment run (-50 ^{o}C to 190 ^{o}C; 190 ^{o}C to -50 ^{o}C; -50 ^{o}C to 160 ^{o}C; held at 160 ^{o}C for 30 mins; 160 ^{o}C to 190 ^{o}C). The thermal information from the second heating cycle of the DSC trace was gained using the data acquisition program Mettler: STAR^e software, where the glass transition temperature (T_g) was taken at the midpoint of the change in heat capacity, and the peak melting temperature (T_m) was determined from the melting endotherm. The crystallinity content (ω_c) of the copolymers was determined by making the assumption that only the PLLA segments contribute to the copolymer crystallinity and thus was based on equation 1.

$$\omega_c(\%) = \left(\frac{\Delta H_m}{\Delta H_m^\circ}\right) \times 100\% \qquad 1$$

Where ΔH_m° is the melting enthalpy of 100 % crystalline PLA with a value of 93 J/g.[22]

Mechanical properties

The tensile properties of the solvent cast P(TMC-co-LLA) films were determined using an INSTRON 5543 (USA) tensile testing machine. A sharp-edged die of ISO-37-4-MET standard (ODC Tooling & Molds, CANADA) was used to cut the samples prior to testing. Sample thicknesses were measured (Kincrome Digital Vernier Caliper) in a minimum of three different areas and the average thickness for the films ranged from 150 - 305 μm. Samples underwent tensile testing both in their dry state and in PBS where pre-cut samples were soaked for 3 days at room temperature to reach equilibrium water uptake before undergoing tensile testing. A 50 N load cell was employed, and the tensile tests were performed using a displacement rate of 50 mm/min. A stress versus strain curve for the samples was generated using the Blue Hill 2 version 2.9 Instron program. The Young's modulus (E), (initial slope), ultimate tensile strength (σ_{max}), and elongation at failure (ε_{break}) for each run was calculated using this program. The stress versus strain data was also re-

plotted in Microsoft Excel to calculate the toughness/strain energy density (area under the stress strain curves from load 0 to failure).

In vitro degradation

P(TMC-co-LLA) solvent cast films underwent *in vitro* degradation in PBS at 37 ºC. Small samples of each copolymer film (approximately 30 mg in weight), in triplicate, were immersed in 30 mL of PBS. The initial weight of each sample was measured using a Mettler Toledo GR-202 balance. The water uptake and mass loss were monitored over a 34 week time period, with the PBS media being changed regularly after the measurements were taken (every 2 - 3 weeks). The solution pH was measured and a maximum change of 0.5 observed during the course of the study. After samples were immersed in PBS for a defined time period, they were removed and lightly dabbed with a Kimwipe to remove excess surface liquid, before being re-weighed. The water uptake was calculated using equation 2

$$Water\ Uptake\ (\%) = \frac{m_w - m_i}{m_i} \times 100\% \qquad 2$$

Where m_i is the initial mass and m_w is the wet mass of the sample.

The water content measurements were done by measuring the dry mass of samples after removing them from the PBS solution and rinsing with MilliQ water before drying to constant weight in a vacuum oven at room temperature. The water content was calculated based on equation 3.

$$Water\ Content\ (\%) = \frac{m_w - m_D}{m_D} \times 100\% \qquad 3$$

Where m_D is the dry mass of the sample.

The mass loss of each sample was calculated using equation 4.

$$Mass\ Loss\ (\%) = \frac{m_D - m_i}{m_i} \times 100\% \qquad 4$$

Results and discussion

Physicochemical properties of the polyester carbonates

A series of statistical P(TMC-co-LLA) polyester carbonate copolymers were synthesised using ROP of TMC and LLA at 130 °C with $Sn(Oct)_2$ as the catalyst based on a previously developed procedure.[21] Six copolymers were produced as indicated in Table 1 and all were obtained in good yields (≥ 83 % yield). The monomer ratio incorporated was determined from ^{1}H NMR and was found to be in close agreement with the feed ratios (within 4 mol %). This outcome is similar to previous studies on synthesis of polyester carbonates via ROP using the same catalyst.[9,21] The sequence length of LLA, $\bar{L}_{LLA}$, evaluated from ^{1}H NMR was found to vary depending on the copolymer composition decreasing with increasing TMC incorporation. A block length of LLA between 14 and 2.8 was calculated for the polymers with compositions between 16 and 49 mol % TMC. These block lengths are greater than expected for a strictly random copolymerisation (eg. $r_{TMC} = r_{LLA} = 1$, theoretical values included in Table 1). This indicates that the reactivity ratio of LLA exceeds that of TMC and correlates with that previously found.[18] The number average molecular weight, $\bar{M}_n$, of the synthesised copolymers ranged from 63 to 31 kg/mol, and showed a consistent decrease in the $\bar{M}_n$ with increasing TMC incorporation, Table 1. This trend is likely due to the presence of impurities such as water and/or other hydroxyl-containing compounds in the TMC monomer, as has been found previously.[9] The presence of such trace impurities, can initiate polymerization which increases the number of the initiation centres, and thus, lowers the $\bar{M}_n$.[9] The molar mass dispersity, $Đ_M$, was found to be similar for all polymers with values between 1.7 and 1.9 in agreement with that previously reported for polyester carbonates produced by ROP using $Sn(Oct)_2$ as catalyst.[23] Recently it was reported that an $\bar{M}_n$ of the same order of magnitude as reported here, could be obtained at the same temperature using a reaction time of 5 h which resulted in dispersities of 1.57 – 1.62.[24]

The thermal properties of the copolymers (listed in Table 1) demonstrate a decreasing T_g with increasing TMC incorporation, in close agreement with the Fox equation and the values for the homopolymers (PLLA T_g = 65 °C [25] and PTMC T_g = -20 °C [26]). This effect of incorporating different amounts of LLA in the amorphous phase on T_g correlates with that previously observed for P(TMC-co-LLA) copolymers.[15] The samples showed a single T_g suggesting the presence of a single amorphous phase. Some of the copolymers did not display a melting endotherm in the DSC heating scan, which can be attributed to slow crystallisation kinetics of polyester carbonates in their second heating cycle.[27] Copolymers incorporating 16,

39 and 49 mol % TMC displayed two characteristic melting endotherms within the range of 130 and 154 ˚C, indicating the formation of two different crystalline fractions.[28] The crystallinity, ω_c, was found to increase with LLA content as evident in Table 1.

Physicochemical properties of the polyester carbonate solvent cast films

The DSC traces of the second heating cycle of the dry films are shown in Figure 1 and Table 2 summarises the thermal properties obtained. The films displayed a significantly reduced T_g compared to the bulk polymers (Table 1) and this is likely due to the plasticisation effect of residual solvent[21,29] which is further supported by the T_g of the first heating cycle, for most copolymers, being lower than for the second heating cycle. This observation is in agreement with reported difficulties in removing traces of chloroform from solvent cast films of statistical P(TMC-co-DLLA) copolymers.[21] In general, the presence of plasticizers swell the amorphous regions which lower the cohesion between the chains and allows these regions to function as flexible elastomeric domains.

The solvent cast films displayed crystallinities between 14 and 1.8 %, decreasing with increasing TMC content (Table 2). All films demonstrated two separate melting endotherms, one around 129 °C and another at around 144 °C. The additional lower temperature T_m present suggests that heating to 190 ^oC (during the first heating cycle) allows the low LLA content chains to crystallise. This result indicates that the copolymer chains have formed distinctly different crystalline regions within the polymer network similar to that observed for the bulk copolymers (Table 1).

Tensile properties of the solvent cast films

Tensile testing of the solvent cast films were performed under ambient (dry) conditions using the as-cast films, as well as (for a selection of samples) under 'wet' conditions, where the films had been pre-soaked in PBS for 3 days at room temperature to reach equilibrium water uptake prior to testing. The equilibrium water uptake was found to be less than 2 wt % for all films studied. No significant changes were observed in the $\bar{M}_n$ or $Đ_M$ values for the as-cast or PBS pre-soaked films compared to the starting materials (data not shown). The tensile properties are listed in Table 3 and Figure 2 shows representative stress-strain curves from each copolymer film tested at both dry and wet conditions. The films were mechanically tested at temperatures below their T_g and they generally exhibited very ductile behaviour with high elongations at break, and low values of E and σ_{max}. From the data it can be seen that the

stiffness of these films is strongly dependent on the copolymer composition, and that higher LLA incorporation results in stiffer films. Films with higher LLA content are also seen to undergo larger loads before becoming irreversibly deformed, have higher strength, and require more energy in order to cause the material to fail. Conversely, these copolymers show the prominent trend of becoming significantly more ductile as the TMC content is increased. These differences appear to be strongly dependent on composition and relates to the T_g and ω_c values, see Table 2. Similar trends have been found by previous for LLA[10,30] and DLLA[30,31] polyester carbonate copolymers. In previous studies on P(TMC-co-LLA) copolymer films prepared either by compression moulding[9] or a combination of solvent casting and compression moulding[5] significantly larger E and σ_{max} values have been observed, while both lower[9] and similar or higher[5] ductility was found. These differences between previous studies and the current work can be attributed to the copolymer films of these previous studies having significantly larger T_g values[5,9] and higher crystallinities[5].

It was found that the film thickness played a significant role in the overall mechanical performance of the solvent cast films tested under 'dry' conditions. For the solvent cast films of P(TMC_{30}-co-LLA_{70}) with different average film thicknesses of 119 μm and 241 μm, it was found that the thinner films are stiffer, have increased strength and are tougher although the elongation at break was not significantly altered. Similar effects were observed in single samples for P(TMC_{39}-co-LLA_{61}) films (data not shown). Such thickness effects are evident for the P(TMC_{27}-co-LLA_{73}) films which have an average thickness of 155 μm, significantly thinner than that of the P(TMC_{21}-co-LLA_{79}) films resulting in their stress-strain curves overlapping as illustrated in Figure 2. These observations are in agreement with previous studies on TMC-containing tri-block copolymer solvent cast films reporting similar results[26] although, in contrast to the current study, this and other studies reported changes in elongation.[26,27,32] It is possible that this film thickness effect is related to the presence of residual solvent in these films with thicker films retaining more residual solvent.

Comparison of the films tested under dry and wet conditions reveals that the wet films generally exhibited an increased stiffness and strength (Table 3 and Figure 2). Furthermore, the copolymer films with low TMC incorporation, P(TMC_{16}-co-LLA_{84}) and P(TMC_{21}-co-LLA_{79}), were tougher when pre-soaked in PBS as compared to when dry, while P(TMC_{30}-co-LLA_{70}) and P(TMC_{39}-co-LLA_{61}) films displayed no change in toughness for the two testing conditions. The ductility for all film compositions was similar across the dry and wet conditions, except for the P(TMC_{39}-co-LLA_{61}) films which displayed significantly greater

elongation under dry conditions. Based on the PBS media having a plasticization effect on polymers in general,[10,21,31,33] a reduction in mechanical properties would be predicted for the films tested under 'wet' conditions. An explanation for the opposite effect being observed in the current study could not be attributed to diffusion of low $\bar{M}_n$ polymer chains from the films, as no changes were observed by GPC after soaking in PBS for 3 days (data not shown). Rather, we attribute the observation to diffusion of the residual organic solvent(s) from the films[21], as well as increased chain mobility provided by the media promoting an annealing effect and facilitating recrystalisation of previously amorphous regions.[28]

In vitro degradation of the solvent cast films

In order to explore the *in vitro* degradation of the P(TMC-co-LLA) solvent cast films over a time frame comparable to previous studies (e.g. 34 weeks),[4,12] partially degraded films (exposed to ambient conditions) were utilised. The resulting molecular weights and molar mass dispersities are listed in Table 4 and it is evident that the partially degraded films displayed up to a threefold reduction in $\bar{M}_n$ compared to the starting polymers (Table 1). The *in vitro* degradation was followed in PBS at 37 °C by determining water content, water uptake and mass loss with the results provided in Figure 3. The water uptake of all P(TMC-co-LLA) films showed very similar behaviour with low water uptake of up to 10 % during the first 64 days (Figure 3A). Similar limited water diffusion into films in the initial stages of degradation has been reported previously for P(TMC-co-LLA) copolymers[4,11,12,14] as well as for P(TMC-co-DLLA) copolymers.[33-35] This observation can be attributed to two inherent physical properties of the homopolymers that are known to affect the degradation behaviour; the extent of hydrophobicity and degree of crystallinity.[15,21,28] The advancing water contact angle of PTMC is reported to be 77° [36] while that for PLLA is 61°.[37] The copolymer films with high TMC content are thus less hydrophilic resulting in a decreased ability to uptake water.[28] In contrast, the copolymers with low TMC content have been found to possess the highest ω_c values (Table 2), which limits uptake of water into the polymers due to the increased density of the crystalline regions as compared to the more accessible amorphous regions.[21,28,34] Direct evaluation of the effect of crystallinity on water uptake was made previously for P(TMC-co-LLA) copolymers with water uptake values of 11 % compared to 2 % reported for the amorphous and crystalline polymers, respectively.[12]

After 79 days of immersion in PBS a significant difference in water uptake between the different compositions can be observed and this becomes pronounced after 99 days (Figure 3A) with the high TMC-content copolymers, P(TMC_{39}-co-LLA_{61}) and P(TMC_{49}-co-LLA_{51}), displaying significantly higher water uptake than the other copolymers. The higher water uptake of these two polymers is mirrored in the water content data at 99 days and is further enhanced with the progress of degradation (Figure 3B). These two compositions reached water content values of 400 and 560 %, respectively, in the late stages of the study. Furthermore, the P(TMC_{30}-co-LLA_{70}) copolymer also demonstrate an increased ability to uptake water from day 113 (Figure 3B). Despite the P(TMC_{27}-co-LLA_{73}) and P(TMC_{30}-co-LLA_{70}) polymers having very similar composition, the P(TMC_{30}-co-LLA_{70}) films display a significantly greater ability to uptake water, reaching maximum water content values of 240 %, compared to only 47 % for the P(TMC_{27}-co-LLA_{73}) films (Figure 3B). The P(TMC_{27}-co-LLA_{73}) films display similar water content values to the films of low TMC content. The observed correlation of increased mol % TMC increasing the ability to uptake water has been reported previously for P(TMC-co-LLA) copolymers[4] and only little discrimination was observed between copolymers with 25 – 17 mol % TMC content.[12]

The thermal properties and polymer composition was examined at two time points during the degradation (Table 5). From this data it can be seen that the P(TMC_{16}-co-LLA_{84}), P(TMC_{21}-co-LLA_{79}) and (TMC_{27}-co-LLA_{73}) copolymers which displayed a limited ability to absorb water (Figure 3) have relatively high T_g and ω_c values of 26 – 28 ^oC and 8.2 – 21 %, respectively. The (TMC_{30}-co-LLA_{70}) copolymers which displayed a somewhat increased ability to absorb water in comparison had a lower T_g of 20 ^oC and ω_c of 5.6 %. Like-wise, the (TMC_{39}-co-LLA_{61}) and (TMC_{49}-co-LLA_{51}) copolymers which displayed the highest ability to absorb water possessed the lowest T_g of 13 and 10 ^oC and ω_c of 3.5 and 0.9 %. Thus, the T_g and ω_c values of P(TMC-co-LLA) copolymers appear to be the dominating properties which dictate the water content profiles after an initial lag period during *in vitro* degradation. These results are consistent with previous studies on P(TMC-co-DLLA) copolymers.[21,34,38]

The mass loss profiles (Figure 3C) show that the copolymers have minimal mass loss of < 8 % until day 99. Low mass loss has previously been seen during the initial weeks of *in vitro* degradation of P(TMC-co-LLA) copolymers.[4,12] After day 99 the copolymers from the current study demonstrate increased mass loss. The P(TMC-co-LLA) solvent cast films with 16 – 27 mol% TMC displayed a direct correlation between mass loss and water uptake. A previous study has likewise found that copolymers of relatively low TMC content (16 – 25

mol%) displayed a correlation between water uptake and mass loss.[12] For the (TMC_{30}-co-LLA_{70}) copolymer of the current study an increased mass loss with increased water uptake was also observed, while for the (TMC_{39}-co-LLA_{61}) and (TMC_{49}-co-LLA_{51}) copolymers there was only relatively small changes in mass loss with increased water uptake. The observation made in the current study for the high TMC content films is similar to that observed for PTMC where increasing the degradation temperature from 37 to 60 ^{o}C resulted in an increase in the water content, however, this difference in water content was found to have no effect on the rate of polymer chain cleavage or on the extent of mass lost by these samples.[28] For the copolymers with 21 – 49 mol% TMC of the current study, it was found that mass loss decreased with increasing crystalline content, Figure 4. This correlation was strong ($R^2 = 0.91$) and related through the equation indicated in Figure 4. A previous *in vitro* degradation study of P(TMC-co-LLA) copolymers have likewise found that mass loss depends on the polymer crystallinity.[4] However, the P(TMC_{16}-co-LLA_{84}) sample of the current study did not follow this trend (predicted near-zero mass loss based on its crystalline content of 21 %). This suggests that the P(TMC_{16}-co-LLA_{84}) polymer degrades via a different mechanism to the other copolymers of this study. A small sample set (n = 1-2) of polymers with same composition (21 and 30 mol% TMC) but higher $\bar{M}_n$ (36 and 34 kg/mol, respectively) were found to display water uptake and mass loss that were indistinguishable from that of their lower $\bar{M}_n$ counterparts. These higher $\bar{M}_n$ polymers were found to have thermal properties that were the same within experimental error of the low $\bar{M}_n$ polymers and this observation thus supports the conclusion that the crystalline content is a dominant factor in the rate of degradation of these polymers.

In addition to water uptake and mass loss studies, the polymer molecular weight distribution was monitored over the course of the *in vitro* degradation with the resulting data displayed in Figure 5 and Table 4. While a mass loss (3.3 – 6.7 %) was observed after 34 days of the *in vitro* degradation study, this was not accompanied by a decrease in $\bar{M}_n$, while for several samples (TMC content of 30 and 39 %) an increase in $\bar{M}_n$ was found (Table 4). This indicates diffusion of water-soluble oligomers and/or low $\bar{M}_n$ fractions into the media.[28] This is further supported by DSC analysis showing that the T_g value increased after 34 days in PBS relative to the initial time point (Tables 5 and 2, respectively) which can be attributed to diffusion of solvent molecules as well as water-soluble low $\bar{M}_n$ fractions of the copolymers. A similar conclusion of slow diffusional loss of oligomers from the polymer

bulk rather than significant hydrolytic chain scission has been made for PTMC in initial stages of degradation.[39]

The T_g value for the copolymers in the current study decreased during *in vitro* degradation from day 34 to day 230 (or 169) as evident in Table 5. This can be related to diffusion of water into the polymer network and subsequent chain scission where the short oligomer chains and the water act as plasticizers and lower the value of T_g.[23,38] Furthermore, the overall decreased in $\bar{M}_n$ (Table 4) also contributes to a lowered T_g. Such changes to T_g has been observed *in vitro* for P(TMC-co-LLA) copolymers[4,12,14] and *in vivo* for P(TMC-co-DLLA) samples with no concomitant change in polymer composition.[40] It was observed that the melting endotherm occurred over a broad temperature range (Table 5) which can be attributed to chains within the polymer network of varying $\bar{M}_n$ forming crystals of different sizes, as previously reported for PLLA.[38] The observed reduction in the starting temperature of the melting transition between day 34 and day 230 (or 169) is likely due to the preferential degradation of the amorphous regions. The degradation reactions lead to the formation of low $\bar{M}_n$ chains which form small crystallites, assisted by the low T_g of the material and annealing from the media; similar effects have been observed for PLLA.[38] The ω_c value remained unchanged between day 34 and day 230 (or 169) for most copolymers of the current study, except for P(TMC_{27}-co-LLA_{73}) and P(TMC_{30}-co-LLA_{70}) where an increase was observed, in agreement with previous observations during degradation studies.[4,10,12,14,28,40-42] This increase in crystalline content indicates that the amorphous regions within these copolymer films are being preferentially degraded over the crystalline regions, or that new crystalline regions form within the polymer network as a result of chain cleavage[28], in agreement with the reduction in the starting temperature of the melting transition described above. A reduction in the end temperature of the melting endotherms indicates that media penetrated into the edge of the larger crystalline domains that were initially present and chain hydrolysis has started and reduced the size of these crystals, as has been reported to occur in semi-crystalline polymers once the majority of amorphous regions have been degraded.[43,44] Considering that the ω_c content remains relatively constant throughout degradation for most copolymer compositions, this is likely occurring in conjunction with formation of new crystalline regions via the re-crystallisation of low $\bar{M}_n$ chains.

The GPC traces in Figure 5 show that the $\bar{M}_n$ decreased with the progress of *in vitro* degradation for all copolymers studied while the date in Table 4 show an increase in the $Đ_M$

values as a function of degradation time. After 99 days of *in vitro* degradation the mass loss and water content remained low (Figure 3), however, the $\bar{M}_n$ had significantly decreased by 36 – 71 % for the P(TMC-co-LLA) copolymers studied (Table 4). This is indicative of chain cleavage resulting in insoluble fractions of degraded polymeric material, which is still of relatively high $\bar{M}_n$ and thus does not diffuse from the film. These observations suggest that these P(TMC-co-LLA) copolymers are undergoing bulk degradation.[28,35] Such observation has previously been made for P(TMC-co-εCL)[28] and P(TMC-co-LLA)[4,12]. For bulk degrading polymers, mass loss occurs at the late stages of degradation, once sufficient water uptake and chain cleavage has taken place, at which time the low $\bar{M}_n$ degraded polymer chains diffuse into the medium.[40] The P(TMC-co-LLA) copolymers in the current study appear to show minimal mass loss of 3.5 – 7.6 % at day 99 when the $\bar{M}_n$ is between 5 – 11 kg/mol, however, the mass loss significantly increases to 13 – 42 % at day 128 when the $\bar{M}_n$ is between 3 – 6 kg/mol (Table 4). Despite overlap in the $\bar{M}_n$ range, it appears that a critical value of approximately 5 - 6 kg/mol is required for these P(TMC-co-LLA) copolymers to reach the onset of rapid decreases in mass. In general, it is found that polymers with higher $\bar{M}_n$ will undergo slower degradation than those of low $\bar{M}_n$.[45] However, the opposite trend has also been reported[45,46] and has in some cases been attributed to reduced crystalline content in the high $\bar{M}_n$ polymers.[45] In the current study, it was found that the change in $\bar{M}_n$ with time was such that both high and low $\bar{M}_n$ polymers approximately halved the $\bar{M}_n$ by day 99 and by day 128 similar $\bar{M}_n$ was obtained regardless of starting $\bar{M}_n$ (Supplementary material, Table S1). This indicates similar rates of degradation at low level of hydration (but slower rate of hydrolysis for the high $\bar{M}_n$ polymers) and faster rate of degradation at high level of hydration (but similar rate of hydrolysis).

Examination of the GPC traces reveals that the films with compositions between 21 and 49 mol% TMC show monomodal GPC traces (Figure 5B – 5F), which suggests that they are undergoing homogeneous bulk degradation.[35] Furthermore, for these copolymers the NMR analysis reveals that the composition and $\bar{L}_{LLA}$ remained relatively constant throughout degradation (Table 5), which indicates that the rate of hydrolysis is similar for the LLA and TMC segments. Previous studies on semicrystalline P(TMC-co-LLA) copolymers with similar composition likewise found a constant copolymer composition and chain microstructure during *in vitro* degradation,[4,14] while amorphous P(TMC-co-LLA) and P(TMC-co-DLLA) copolymers showed preferential degradation of the LLA segments.[4,12,33,34,40] From the GPC trace of the P(TMC_{16}-co-LLA_{84}) film displayed in Figure

5A, it can be seen that this polymer developed a bimodal $\bar{M}_n$ distribution at the later stages of degradation. Such bimodal $\bar{M}_n$ distributions have previously been seen in intrinsically semi-crystalline polymers[40,41] and is interpreted in terms of the hydrolytic cleavage of the ester and carbonate bonds forming acidic degradation products, causing an auto-catalytic effect within the interior of the sample where the medium has limited buffering effect. These different degradation environments in the centre of the sample and at the surface increases the $Đ_M$ value and causes development of a low $\bar{M}_n$ shoulder, being described as an auto-catalysed heterogeneous bulk degradation mechanism.[28,42] This observation correlates with the P(TMC_{16}-co-LLA_{84}) polymer displaying much higher mass loss than that predicted from its crystallinity as described above.

NMR analysis of the P(TMC_{16}-co-LLA_{84}) film showed that the LLA content significantly increased by 5 mol % and the $\bar{L}_{LLA}$ increased by an average of 3 units during degradation from day 34 to day 230 (Table 5). This data suggests that the carbonate linkages in the TMC segments are more susceptible to hydrolysis than the ester linkages in the LLA segments within the P(TMC_{16}-co-LLA_{84}) film. A similar observation regarding relative rates of degradation for TMC and LLA segments has previously been seen in P(TMC-co-LLA) copolymers.[4,11] The fact that only the P(TMC_{16}-co-LLA_{84}) copolymer of the current study displays heterogeneous bulk degradation while the remaining copolymers show homogeneous bulk degradation is likely due to the high LLA content in conjunction with the low water content limiting diffusion of the acidic degradation products from the bulk.

Conclusion

In both the dry and wet state, the tensile properties of solvent cast films of P(TMC-co-LLA) were composition dependent and highly tuneable, with copolymers with high LLA content displaying enhanced stiffness, strength and toughness, while the TMC moieties promoted greater ductility. Residual solvent in solvent-cast P(TMC-co-LLA) films impacted their mechanical properties and could be related to the observed T_g values. Samples tested after pre-soaking in PBS generally displayed higher modulus, ultimate tensile strength and toughness, while the elongation at break did not change significantly, spanning a range of 356 to 1287 %. In addition, sample thickness was found to affect the mechanical properties of these copolymer films, with thinner films displaying enhanced E, σ_{max} and toughness compared to thicker films.

Exposure to ambient conditions for extended periods of time resulted in lowered $\bar{M}_n$ as well as an initial mass loss of 3.3 – 6.7 %, attributed to leaching of water-soluble oligomers and/or low $\bar{M}_n$ species. An induction period of 64 days of the *in vitro* degradation study was observed during which the water content was minimal (< 10 %) for all copolymers and attributed to inherent properties of the polymers limiting water diffusion into the polymer network. The water content in the late stages of degradation was found to be compositionally dependent and correlated with T_g and inherent crystallinity of the copolymers. The water content varied 10 fold between samples while mass loss was similar for all copolymers. Bulk degradation was identified as the dominant degradation mechanism, based on a large reduction in $\bar{M}_n$ taking place before any significant water uptake or mass loss occurred. Specifically, copolymer films with 21 or greater mol% TMC were found to undergo homogeneous bulk degradation, identified by monomodal GPC traces throughout degradation and a similar rate of hydrolysis for the LLA and TMC segments. In contrast, the P(TMC_{16}-co-LLA_{84}) films underwent heterogeneous bulk degradation, identified by the development of bimodal GPC traces and for this copolymer preferential degradation of the TMC segments was found. When comparing our results to other studies, it appears that the relative rate of degradation of the lactide or carbonate segments is related to the crystallinity of the film. An $\bar{M}_n$ value of 5-6 kg/mol was identified as a threshold before substantial water uptake and mass loss could be observed.

This study has extended the understanding of mechanical properties and *in vitro* degradation of P(TMC-co-LLA) copolymers, highlighting that these properties are not only compositionally dependent but also affected by other factors, of which the T_g and crystallinity appear to be very dominant.

Acknowledgements

The authors would like to thank Dr Grant Edwards for assistance with tensile testing. Funding for the International Biomaterials Research Alliance was provided by the Queensland State Government, under the National and International Research Alliance Scheme. Access to equipment of the Queensland node of the Australian National Fabrication Facility, a company established under the National Collaborative Research Infrastructure Strategy to provide nano- and microfabrication facilities for Australia's researchers, is also acknowledged. J Cork wishes to thank the Australian government for an Australian Postgraduate Award.

References

1 D. J. Darensbourg, W. Choi and C. Richers, *Macromolecules,* 2007, 40, 3521-3523.

2 D. W. Grijpma, A. J. Nijenhuls, P. G. T. van Wijk and A. J. Pennings, *Polymer Bull.* 1992, 29, 571-578.

3 A. P. Pego, A. A. Poot, D. W. Grijpma and J. Feijen, *J. Biomater. Scie., Polym. Ed.*, 2001, 12, 35-53.

4 J. Hua, K. Gebarowska, P. Dobrzynski, J. Kasperczyk, J. Wei and S. J. Li, *Polym. Sci., Part A: Polym. Chem.*, 2009, 47, 3869-3879.

5 Y. Han, X. Jin, J. Yang, Z. Fan, Z. Lu, Y. Zhang and S. Li, *Polym. Eng. Sci.*, 2012, 52, 741-750.

6 J. Yang, Y. Qin, M. Yuan, J. Xue, J. Cao, Y. Wu and M.Yuan, *Int. J. Biol. Macromolecules,* 2013, 62, 411-417.

7 P. Plikk, S. Malberg and A.-C. Albertsson, *Biomacromolecules*, 2009, 10, 1259-1264.

8 S. Mukherjee, C. Gualandi, M. L. Focarete, R. Ravichandran, J. R. Venugopal, M. Raghunath and S. Ramakrishna, *J. Mater. Sci. Mater. Med.*, 2011, 22, 1689-1699.

9 E. Ruckenstein and Y. Yuan. *J. Appl. Polym. Sci.*, 1998, 69, 1429-1434.

10 D. W. Grijpma and A.J. Pennings, *Macromol. Chem. Phys.*, 1994, 195, 1649-63.

11 V. Truong, I. Blakey and A. K.Whittaker, *Polym. Prepr. (Am. Chem. Soc., Div. Polym. Chem.)*, 2008, 49, 1097-1098.

12 Y. Han, Z. Fan, Z. Lu, Y. Zhang and S. Li, *Macromol. Mater. Eng.*, 2012, 297, 128-135.

13 J. Kasperczyk, K. Jelonek, K. Gebarowska, P. Dobrzynski and A. Somola, *J. Control. Release*, 2001, 152, e1-e132.

14 Y.-L. Li, S. Li, L.-J. Ji, B. He and Z.-W. Gu, *Chinese J. Polym. Sci.*, 2013, 31, 966-973.

15 D. W. Grijpma and A. J. Pennings, *Macromol. Chem. Phys.*, 1994, 195, 1633-47.

16 Q. Guo, Z. Lu, Y. Zhang, S. Li and J. Yang, *Acta Biochim. Biophys. Sin.*, 2011, 43, 433-440.

17 J. Yang, F. Liu, S. Tu, Y. Chen, X. Luo, Z. Lu, J. Wei and S. Li, *J. Biomed. Mater. Res. Part A*, 2010, 94A, 396-407.

18 B. L. Dargaville, C. Vaquette, H. Peng, F. Rasoul, Y. Q. Chau, J. J. Cooper-White, J. H. Campbell and A. K. Whittaker, *Biomacromolecules*, 2011, 12, 3856-3869.

19 B. L. Dargaville, C. Vaquette, F. Rasoul, J. J. Cooper-White, J. H. Campbell and A. K. Whittaker, *Acta Biomaterialia*, 2013, 9, 6885-6897.

20 K. Jelonek, J. Kasperczyk, S. Li, P. Dobrzynski and B. Jarzabek, *Int. J. Pharm.*, 2011, 414, 203-209.

21 A. P. Pego, A. A. Poot, D. W. Grijpma and J. Feijen, *J. Mater. Sci. Mater. Med.*, 2003, 14, 767-773.

22 E. W. Fischer, H. J. Sterzel and G. Wegner, *Kolloid-Zu Z-Polymer*, 1973, 251, 980-990.

23 C. A. P. Joziasse, H. Veenstra, M. D. C. Topp, D. W. Grijpma and A. J. Pennings, *Polymer*, 1998, 39, 467-473.

24 H. Li, J. Chang, Y. Qin, Y. Wu, M. Yuan and Y. Zhang, *Int. J. Mol. Sci.*, 2014, 15, 2608-2621.

25 M. Zuideveld, C. Gottschalk, H. Kropfinger, R. Thomann, M. Rusu and H. Frey, *Polymer*, 2006, 3740-3746.

26 Z. Zhang, D. W. Grijpma and J. Feijen, *J. Mater. Sci. Mater. Med.*, 2004, 15, 381-385.

27 J.-H. Kim and J. H. Lee, *Macromol. Res.*, 2002, 10, 54-59.

28 A.-C. Albertsson and M. Eklund, *J. Appl. Polym. Sci.*, 1995, 57, 87-103.

29 T. Tyson, A. Finne-Wistrand and A.-C. Albertsson, *Biomacromolecules*, 2009, 10, 149-154.

30 Z. Zhang, D. W. Grijpma and J. Feijen, *Macromol. Chem. Phys.*, 2004, 205, 867-875.

31 B. Buchholz, *J. Mater. Sci. Mater. Med.*, 1993, 4, 381-388.

32 J.-H. Kim and J. H. Lee, *Polym. Journal*, 2002, 34, 203-208.

33 A. P. Pego, A. A. Poot, D. W. Grijpma and J. Feijen, *J. Control. Release*, 2003, 87, 69-79.

34 A. P. Pego, A. A. Poot, D. W. Grijpma and J. Feijen, *Macromol. Biosci.*, 2002, 2, 411-419.

35 C. Jie and K. J. Zhu, *Polym. Int.*, 1997, 42, 373-379.

36 Z. Zhang, R. Kuijer, S. K. Bulstra, D. W. Grijpma and J. Feijen, *Biomaterials*, 2006, 27, 1741-1748.

37 K. Gwang-Hoe and J. Jinho, *Fibres Polym.*, 2008, 9, 674-678.

38 S. M. Li, H. Garreau and M. Vert, *J. Mater. Sci. Mater. Med.*, 1990, 1, 198-206.

39 K. J. Zhu, R. W. Henderson, K. Jensen and C. G. Pitt, *Macromolecules*, 1991, 24, 1736-1740.

40 A. P. Pego, M. J. A. Van Luyn, L. A. Brouwer, P. B. van Wachem, A. A. Poot, D. W. Grijpma and J. Feijen, *J. Biomed. Mater. Res. Part A*, 2003, 67A, 1044-1054.

41 S. M. Li, H. Garreau and M. Vert, *J. Mater. Sci. Mater. Med.*, 1990, 1, 123-130.

42 Y. Lemmouchi, E. Schacht, P. Kageruka, R. De Deken, B. Diarra, O. Diall and S. Geerts, *Biomaterials*, 1998, 19, 1827-1837.

43 H. Antheunis, J.-C. van der Meer, M. de Geus, W. Kingma and C. E. Koning, *Macromolecules*, 2009, 42, 2462-2471.

44 J. Wang, F. Dong, G. Huang and Y. Jia, *Carbohydrate Polym.*, 2011, 86, 226-230.

45 H. K. Makadia and S. J. Siegel, *Polymers*, 2011, 3, 1377-1397.

46 X. S. Wu and N. Wang, *J. Biomater. Sci. Polymer Edn.*, 2001, 12, 21-34.

Table 1. Physicochemical charcterisation by NMR, GPC and DSC analysis of the as-prepared P(TMC-co-LLA) copolymers

Feed ratio (TMC/LLA)	Copolymer	$\bar{L}_{LLA}$		$\bar{M}_n$ (kg/mol)	$Đ_M$	T_g (°C)	T_m (°C)	ω_c (%)
		observed	theoretical					
15/85	P(TMC_{16}-co-LLA_{84})	14	6.3	63	1.9	44	130, 154	7.4
20/80	P(TMC_{21}-co-LLA_{79})	8.1	4.8	59	1.8	42	-	-
23/77	P(TMC_{27}-co-LLA_{73})	8.1	3.7	49	1.7	37	-	-
30/70	P(TMC_{30}-co-LLA_{70})	5.3	3.3	42	1.9	39	-	-
40/60	P(TMC_{39}-co-LLA_{61})	3.6	2.6	33	1.9	26	134, 149	3.2
50/50	P(TMC_{49}-co-LLA_{51})	2.8	2.0	31	1.8	14	134, 147	1.9

T_g, T_m & ω_c were obtained from the 2nd heating cycle of the DSC thermogram; (-) = not detected.

Table 2. Thermal properties of dry solvent cast films

Copolymer	T_g (°C)	T_m (°C)	ω_c (%)
P(TMC_{16}-co-LLA_{84})	21	128, 147	14
P(TMC_{21}-co-LLA_{79})	21	131, 153	6.2
P(TMC_{27}-co-LLA_{73})	13	125, 138	4.9
P(TMC_{30}-co-LLA_{70})	10	127, 140	2.5
P(TMC_{39}-co-LLA_{61})	12	131, 144	3.1
P(TMC_{49}-co-LLA_{51})	7	132, 145	1.8

T_g, T_m & ω_c were obtained from the 2nd heating cycle of the DSC thermogram

Table 3. Tensile properties (± standard deviation) of solvent cast films

Copolymer	Condition[a]	Thickness (µm)	E (MPa)	σ_{max} (MPa)	ε_{break} (%)	Toughness (mJ/mm^3)
P(TMC$_{16}$-co-LLA$_{84}$)	dry[b]	192 (21)	271 (36)	15.5 (1.2)	356 (20)	43 (4)
	wet[c]	220 (21)	330 (59)	19.8 (1.5)	381 (29)	60 (7)
P(TMC$_{21}$-co-LLA$_{79}$)	dry[d]	185 (23)	42 (3)	8.2 (0.5)	365 (67)	25 (6)
	wet[c]	223 (26)	122 (32)	13.5 (1.5)	423 (29)	41 (5)
P(TMC$_{27}$-co-LLA$_{73}$)	dry[e]	155 (5)	89 (14)	8.8 (0.4)	446 (31)	30 (3)
P(TMC$_{30}$-co-LLA$_{70}$)	dry[d]	119 (16)	47 (28)	5.4 (0.5)	570 (39)	23 (1)
	dry[c]	241 (35)	18 (8)	3.0 (0.4)	647 (78)	16 (3)
	wet[f]	155 (18)	34 (8)	7.3 (0.9)	545 (31)	25 (3)
P(TMC$_{39}$-co-LLA$_{61}$)	dry[c]	176 (10)	7.3 (1.4)	1.6 (0.2)	1028 (109)	14 (3)
	wet[e]	148 (19)	24 (3)	3.2 (0.5)	639 (24)	16 (1)
P(TMC$_{49}$-co-LLA$_{51}$)	dry[c]	205 (38)	2.8 (0.2)	0.6 (0.1)	1287 (170)	5 (2)

a: 'dry' refers to testing under ambient conditions, 'wet' refers to testing after immersion of the film in PBS for 3 days; b: n = 4; c: n = 5; d: n = 3; e: n = 6; f: n = 7

Table 4. Number average molecular weight and dispersity of solvent cast films during the *in vitro* degradation study

Copolymer	Property	Time (days)					
		0	34	99	128	169	230
P(TMC$_{16}$-co-LLA$_{84}$)	$\bar{M}_n$ (kg/mol)	21	22	11	5	4	3
	$Đ_M$	1.9	1.9	2.3	3.5	3.3	3.2
P(TMC$_{21}$-co-LLA$_{79}$)	$\bar{M}_n$ (kg/mol)	16	18	8	6	4	3
	$Đ_M$	2.1	2.1	2.9	3.0	2.8	2.9
P(TMC$_{27}$-co-LLA$_{73}$)	$\bar{M}_n$ (kg/mol)	21	22	6	5	4	-
	$Đ_M$	1.9	1.9	2.8	2.8	2.9	-
P(TMC$_{30}$-co-LLA$_{70}$)	$\bar{M}_n$ (kg/mol)	11	17	7	4	3	3
	$Đ_M$	2.4	1.9	2.6	2.8	2.7	2.4
P(TMC$_{39}$-co-LLA$_{61}$)	$\bar{M}_n$ (kg/mol)	13	16	5	3	3	3
	$Đ_M$	2.0	1.8	2.5	2.8	2.4	2.2
P(TMC$_{49}$-co-LLA$_{51}$)	$\bar{M}_n$ (kg/mol)	18	17	8	3	4	3
	$Đ_M$	1.8	1.8	1.6	2.2	2.1	2.0

(-) = not determined

Table 5. Physicochemical properties of solvent cast films during the *in vitro* degradation study

Copolymer	Time (days)	T_g (°C)	T_m [a] (°C)	ω_c (%)	TMC (mol %)	$\bar{L}_{LLA}$
P(TMC_{16}-co-LLA_{84})	34	34.5	103-159	20	18	12
	230	26	103-139	21	13	15
P(TMC_{21}-co-LLA_{79})	24	37	119-164	8.2	22	8
	230	28	103-152	8.2	21	9
P(TMC_{27}-co-LLA_{73})	34	34	106-157	6.7	26	7
	169	27	103-148	9.1	25	8
P(TMC_{30}-co-LLA_{70})	34	29	121-155	2.9	31	5
	230	20	103-143	5.6	31	6
P(TMC_{39}-co-LLA_{61})	34	23.5	125-155	3.1	39	4
	230	13	103-139	3.5	40	4
P(TMC_{49}-co-LLA_{51})	34	17	130-156	1.5	49	3
	230	10	116-137	0.9	51	3

All DSC values (T_g, T_m & ω_c) were obtained from the 2nd heating cycle of the DSC thermogram. a: Values for T_m are reported as a range as multiple peaks were observed.

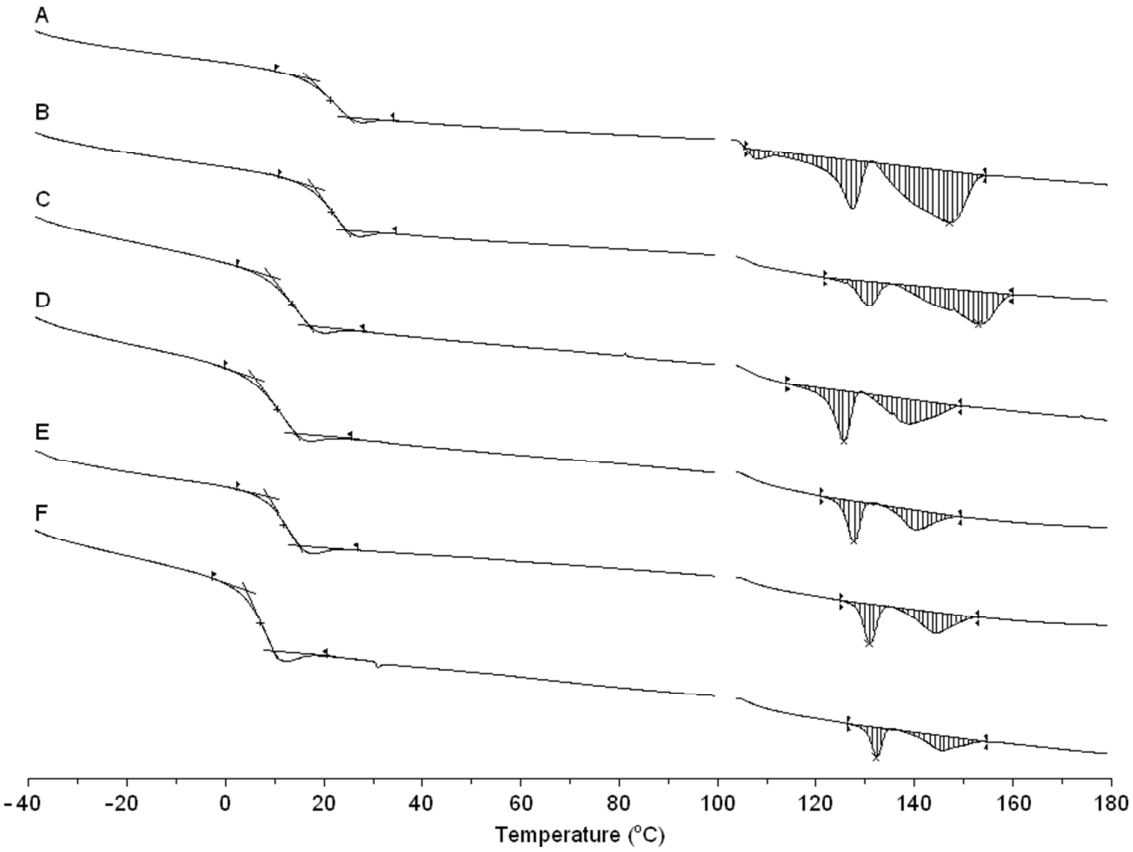

Figure 1. DSC theromgrams of solvent cast films in their second heating scan displaying segments 3 and 5 of the 5-segment run. A: P(TMC_{16}-co-LLA_{84}); B: P(TMC_{21}-co-LLA_{79}); C: P(TMC_{27}-co-LLA_{73}); D: P(TMC_{30}-co-LLA_{70}); E: P(TMC_{39}-co-LLA_{61}); F: P(TMC_{49}-co-LLA_{51}). Up is exothermic; down is endothermic.

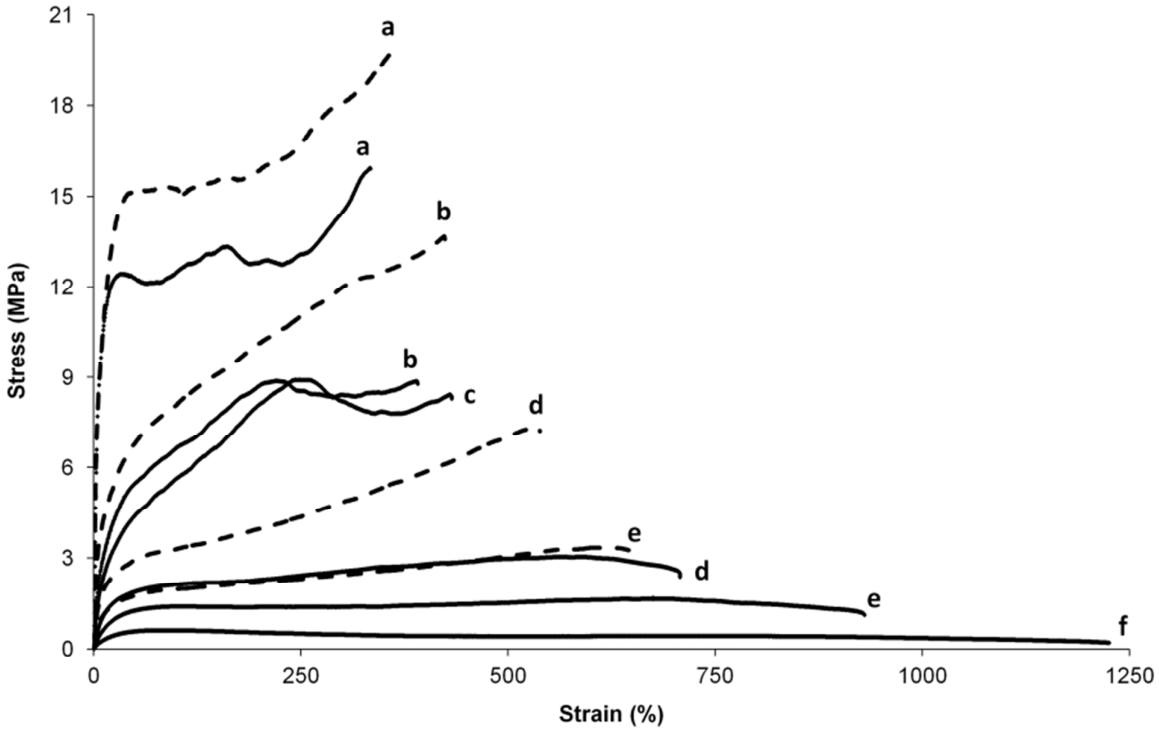

Figure 2. Stress-strain curves of solvent cast samples measured under dry conditions (solid line) and wet conditions (dashed line); a: P(TMC_{16}-co-LLA_{84}); b: P(TMC_{21}-co-LLA_{79}); c: P(TMC_{27}-co-LLA_{73}); d: P(TMC_{30}-co-LLA_{70}); e: P(TMC_{39}-co-LLA_{61}); f: P(TMC_{49}-co-LLA_{51}).

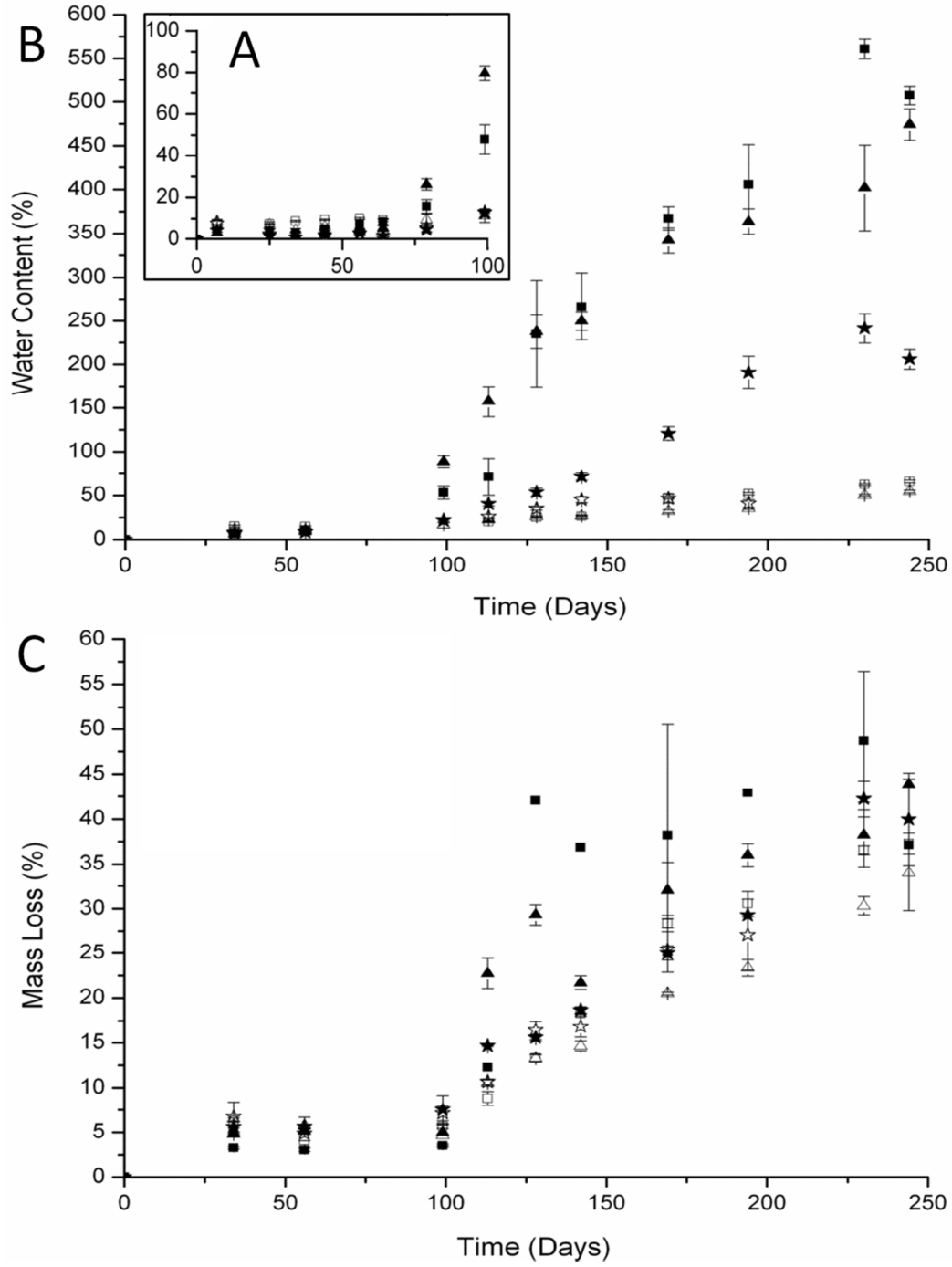

Figure 3. Data for *in vitro* degradation of P(TMC-co-LLA) solvent cast films. A: Water uptake versus time in days; B: water content; C: mass loss. □: P(TMC_{16}-co-LLA_{84}); △: P(TMC_{21}-co-LLA_{79}); ☆ : P(TMC_{27}-co-LLA_{73}); ★: P(TMC_{30}-co-LLA_{70}); •: P(TMC_{39}-co-LLA_{61}); ■: P(TMC_{49}-co-LLA_{51}). Error bars is standard error of the mean.

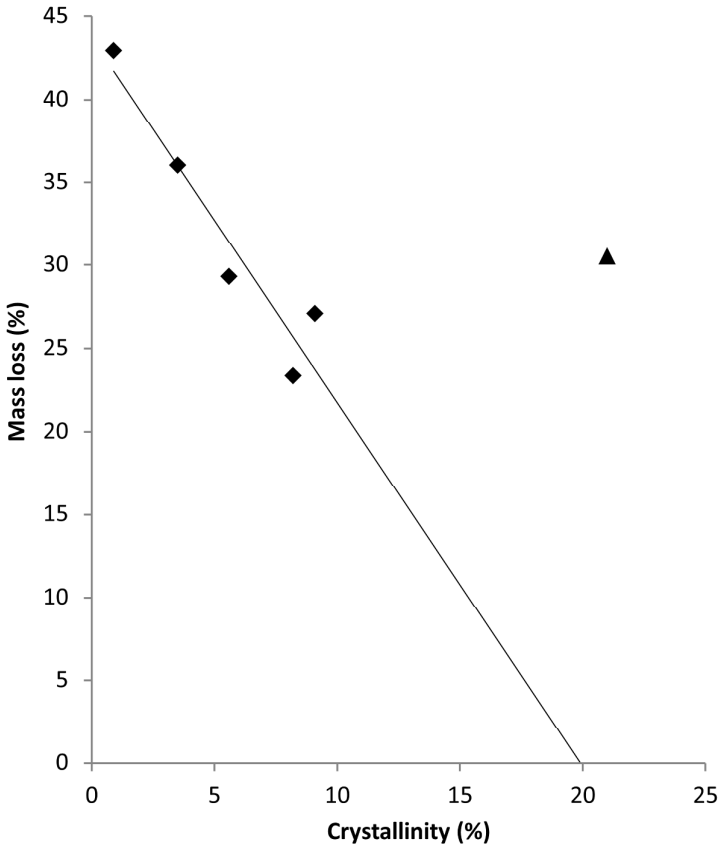

Figure 4. Mass loss and crystallinity correlation. ◆: P(TMC-co-LLA) copolymers with between 21 and 49 mol% TMC content; ▲: P(TMC_{16}-co-LLA_{84}) copolymer. The linear fit to the data for the 21 to 49 mol% TMC content polymers is given by: Mass loss (%) = -2.2 × Crystallinity (%) + 43.7, and an $R^2 = 0.91$.

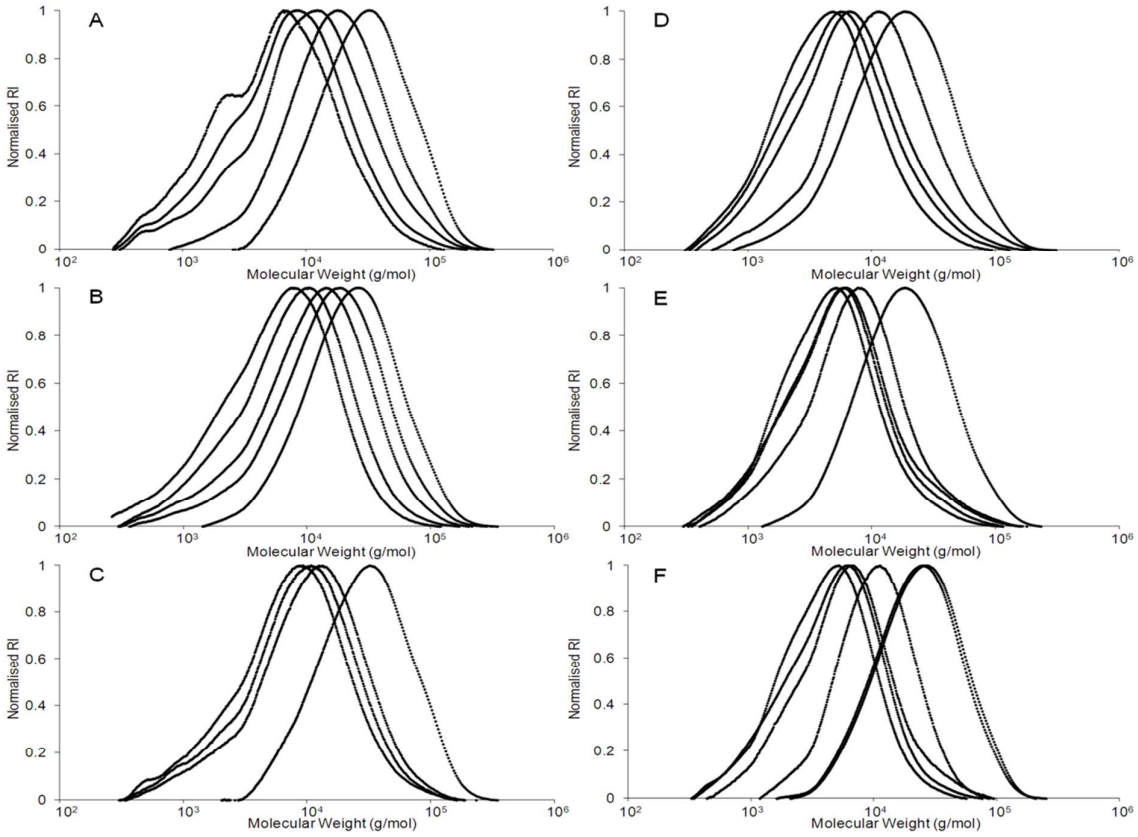

Figure 5. GPC traces of P(TMC-co-LLA) solvent cast films during *in vitro* degradation study. A: P(TMC_{16}-co-LLA_{84}); B: P(TMC_{21}-co-LLA_{79}); C: P(TMC_{27}-co-LLA_{73}); D: P(TMC_{30}-co-LLA_{70}); E: P(TMC_{39}-co-LLA_{61}); F: P(TMC_{49}-co-LLA_{51}). For each series of GPC traces from right to left are from the time points 0, 99, 128, 196 and 230 days.

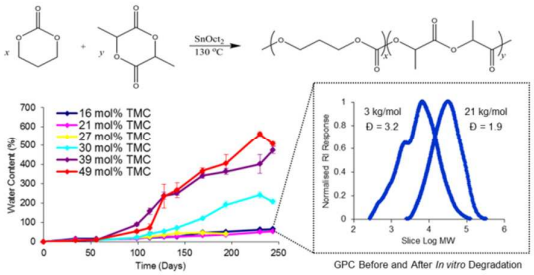

The degradation mechanism of P(TMC-co-LLA) films was dependent on the LLA content and found to transition from heterogeneous to homogeneous bulk degradation.